Instabilities and Transition in Magnetohydrodynamic Flows in Ducts with Electrically Conducting Walls

Maxime Kinet* and Bernard Knaepen
Université Libre de Bruxelles, Faculté des Sciences, Physique Statistique et des Plasmas, Campus Plaine CP231, B-1050 Bruxelles, Belgium

Sergei Molokov
Applied Mathematics Research Centre, Coventry University, Priory Street, Coventry CV1 5FB, United Kingdom
(Received 1 April 2009; published 7 October 2009)

This Letter presents a numerical study of a magnetohydrodynamic flow in a square duct with electrically conducting walls subject to a uniform, transverse magnetic field. Two regimes of instability and transition of Hunt's jets at the walls parallel to the magnetic field have been identified. The first one occurs for relatively low values of the Reynolds number Re and is associated with weak, periodic, counterrotating vortices discovered previously in linear stability studies. The second is a new regime taking place for higher values of Re. It is associated with trains of small-scale vortices enveloped into larger structures, and involves partial detachment of jets from parallel walls. Once this regime sets in, the kinetic energy of perturbations increases by 2 orders of magnitude.

DOI: 10.1103/PhysRevLett.103.154501 PACS numbers: 47.20.−k, 47.27.Cn, 47.27.ek, 52.65.Kj

Introduction.—Liquid metal flows are of great importance for blankets of nuclear fusion reactors, such as tokamaks [1]. The role of the blankets is to breed tritium, to extract energy from the burning plasma, or both. The blankets are composed of ducts of rectangular cross section, where liquid metal, typically lithium or its alloys, flows in the presence of a high, 5–10 T magnetic field. The ducts comprising the blanket usually have electrically conducting walls even if sometimes they are coated with an imperfectly electrically insulating material. Instabilities, transition, and turbulence in such flows are very beneficial as they induce mixing of the fluid and thus more efficient heat and mass transfer. These issues are crucial to determine whether a particular design of a blanket can be realized in practice.

Unfortunately, the understanding of the mechanisms of instabilities and transition in the presence of high magnetic fields is almost exclusively limited to flows in channels rather than ducts, i.e., to flows between two infinite parallel plates (see, e.g., [2,3] and references therein). In channels transition takes place according to the bypass scenario in which streamwise vortices play a key role. These studies, however, are mainly of academic significance as the sidewalls of the ducts always affect the flows in a major way, even more so than in nonconducting fluids.

In the presence of a strong, transverse magnetic field, the flow in rectangular ducts with conducting walls becomes highly anisotropic with an almost flat core, exponential Hartmann layers at the walls transverse to the magnetic field [4], and Hunt's jets [5,6] at the walls parallel to the field (Fig. 1). This anisotropy is owed to the magnetohydrodynamic (MHD) interaction, which shapes the velocity profile by means of the Lorentz force. The jets are of particular importance for the flow balance as they carry either all or part of the volume flux depending on the ratio of the electrical conductances of the Hartmann walls and parallel walls to the conductance of the fluid.

The velocity profile shown in Fig. 1 is highly unstable even for moderate values of the Reynolds number Re and high values of the Hartmann number Ha [7–11]. According to the asymptotic linear stability theory developed previously by Ting *et al.* [7], the critical value of Re for the instability of this type tends to a constant, independent of Ha as Ha $\to \infty$. The small-scale, Ting and Walker's (TW) vortices is not the only possible type of instability, how-

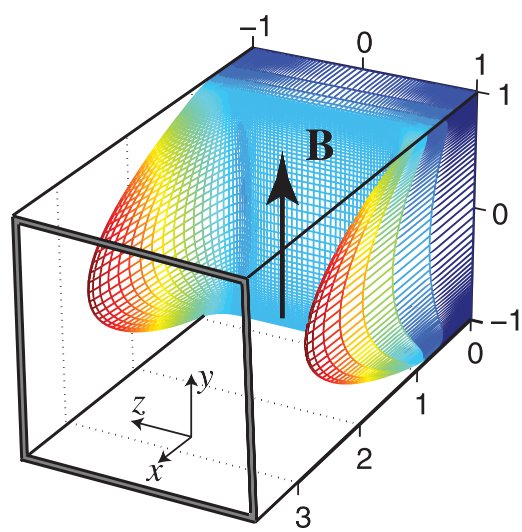

FIG. 1 (color online). Base velocity profile for a square duct with thin conducting walls for $c = 0.5$ and for $\mathrm{Ha} = 200$.

 © 2009 The American Physical Society

ever. Priede *et al.* [11] demonstrated a rich variety of instability patterns in Hunt's flow (for perfectly conducting Hartmann walls and electrically insulating parallel walls) as Ha increases from zero. In particular, they have shown that for low values of Ha instability occurs in the form of streaks occupying the whole duct cross section, while TW vortices are most unstable for Ha > 46.

Here, using numerical simulations, we go beyond the linear stability threshold and present a new type of instability of Hunt's jets, which is associated with their partial detachment from the parallel walls. Once this pattern sets in, the energy of perturbations grows by 2 orders of magnitude. This type of instability persists for a wide range of Re and appears to be a common feature of MHD flows with Hunt's jets.

Governing equations.—Consider the flow of a liquid metal in a square duct whose main axis is in the x direction in the presence of a magnetic field with induction B_0 applied in the y direction (see Fig. 1). We assume that the fluid is incompressible and that the magnetic field induced by the fluid motion can be neglected so that the quasistatic approximation holds [1]. The problem is governed by the set of dimensionless equations,

$$\mathrm{Re}\,[\partial_t \mathbf{u} + (\mathbf{u}\cdot\nabla)\mathbf{u}] = -\mathrm{Ha}^2\nabla p + \nabla^2\mathbf{u} + \mathrm{Ha}^2\mathbf{J}\times\mathbf{B}, \tag{1}$$

$$\nabla\cdot\mathbf{u} = 0, \qquad \nabla\cdot\mathbf{J} = 0, \qquad \mathbf{J} = -\nabla\phi + \mathbf{u}\times\mathbf{B}, \tag{2}$$

which express the conservation of momentum, mass and electric charge, and Ohm's law, respectively. The mass flux is maintained constant. The velocity $\mathbf{u} = (u_1, u_2, u_3)$, the magnetic field $\mathbf{B}$, the current density $\mathbf{J}$, the pressure p, the electric potential ϕ, and time t are normalized by U, B_0, $\sigma U B_0$, $\sigma\delta B_0^2 U$, $\delta U B_0$, and τ_u respectively, U being the bulk velocity, δ half the width of the duct, σ the electrical conductivity of the fluid, and $\tau_u = \delta/U$ the eddy turnover time. The Reynolds number, $\mathrm{Re} = U\delta/\nu$, expresses the ratio of inertial to viscous forces, while the square of the Hartmann number, $\mathrm{Ha} = \delta B_0(\sigma/\rho\nu)^{1/2}$, measures the relative strength of the electromagnetic forces versus viscous ones.

The boundary conditions are the no-slip- and thin-conducting-wall conditions at each solid wall:

$$\mathbf{u} = 0, \qquad \mathbf{J}\cdot\mathbf{n} = c\nabla_\tau^2\phi \quad \text{at } y = \pm 1, \qquad z = \pm 1, \tag{3}$$

where $\mathbf{n}$ is the outward normal unit vector to a wall, ∇_τ^2 is the Laplace operator in the plane of the wall, $c = \sigma_w\delta_w/\sigma\delta$ is the wall conductance ratio, and σ_w and δ_w are the electrical conductivity and thickness of the wall, respectively.

The commonly used thin-conducting-wall condition [1] is based on the assumption that the wall is thin compared to the duct dimensions, i.e., $\delta_w \ll \delta$. This implies that the wall electric currents flow strictly in the plane of the wall but are allowed to enter (leave) the wall from (into) the fluid.

Results.—The problem defined by Eqs. (1)–(3) has been solved using the CDP code developed at the Center for Turbulence Research (Stanford/NASA-Ames) and upgraded to model MHD flows. This code implements a finite volume discretization on a collocated mesh. It is based on a fractional step method, second order in space and time, and has been extensively tested in turbulent flows. The Lorentz force is discretized using a consistent and conservative formulation (see [12–14] for details).

Simulations have been performed with periodic boundary conditions in the streamwise direction, starting from an initial condition consisting of random noise. After a transient period the flow reaches a statistically steady state, which is then analyzed as described below.

The results are presented for a square duct with $c = 0.5$, which corresponds to all walls being quite good conductors, for Ha $= 200$, and for eight values of Re in the range 10^3–10^4. Owing to the limit on computational resources it has not been feasible to perform calculations for higher values of Ha $\sim 10^3$–10^4 characteristic for fusion blankets, as this would require a much higher numerical resolution. Nevertheless, the value of Ha $= 200$ is sufficiently high for the base velocity profile to exhibit a distinct core, Hartmann layers and two well-separated Hunt's jets in the parallel layers (Fig. 1). For Ha $= 200$ the value of the core velocity is 0.85, while the maximum velocity of the jet is 2.7. For all the values of Re considered here, $\mathrm{Re}_{\max}/\mathrm{Ha} \le 50$, which implies that the Hartmann layers remain stable as they are in all the elements of fusion blankets [4]. The instability comes from the shear and the inflectional nature of the mean velocity profile in the jet region.

The length of the computational domain has been set to 4π, and the resolution to $512 \times 100 \times 100$ grid points in the x, y, and z direction, respectively. This ensured that both the Hartmann layers and parallel layers are fully resolved. Care has been taken to make the flow pattern independent of the length of the computational domain.

The velocity is split into the mean, $\mathbf{U}$, and the fluctuating, $\mathbf{u}'$, parts, where $\bar{\mathbf{u}} = \mathbf{U}$, $\bar{\mathbf{u}}' = 0$. The overbar denotes time averaging. Similar definitions hold for other flow quantities.

The three components of the kinetic energy density of perturbations are

$$e_i = \frac{1}{V}\int_V u_i'^2 dV, \qquad i = 1, 2, 3, \tag{4}$$

where V is the volume of the computational domain. Their mean values are shown in Fig. 2 against Re. For Re $= 1000$ (not shown on the graph) the intensity of perturbations remains at the level of the numerical error $\sim 10^{-16}$ even for a very long calculation of up to $t = 2000$. The flow remains laminar with no signs of instability. For $2500 \le \mathrm{Re} \le 3500$ the value of $\bar{e}_i$ for all three components in-

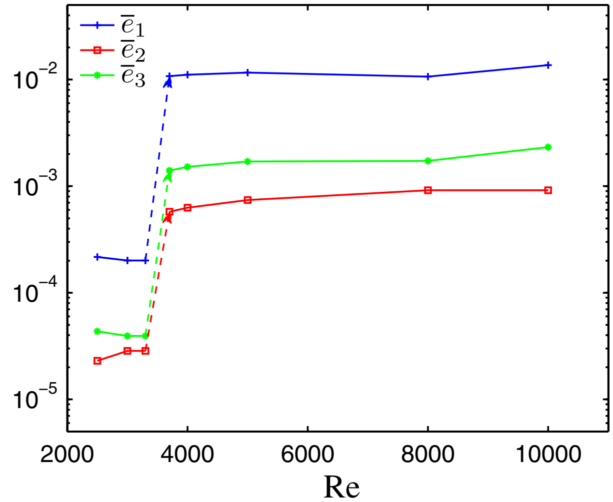

FIG. 2 (color online). Kinetic energy density of perturbations averaged in time as a function of Re.

creases to 10^{-5}–10^{-4}, while for Re ≥ 3700 it jumps up by 2 orders of magnitude. This jump is accompanied by the reduction of the maximum mean velocity and by the thickening of the jet as shown in Fig. 3. The first instability is associated with TW vortices, while the second with a new type of instability involving partial detachment of jets from parallel walls.

The instability for $2500 \leq \mathrm{Re} \leq 3500$ is characterized by two rows of small-scale, almost periodic vortices, one at each parallel wall. Each row consists of a succession of clockwise (CW) and counterclockwise (CCW) rotating vortices. Their magnitude is so small that they do not affect the mean velocity profile, and thus this regime is close to being linear.

For Re ≥ 3700 a new type of instability occurs. The instability has the form of long, essentially traveling waves, containing trains of small-scale vortices enveloped into large structures and interrupted by partial detachment of the jets from parallel walls (Fig. 4). The small-scale vortices evolve in time but the large-scale structure propagates downstream without changing its shape. The intensity of disturbances increases by 2 orders of magnitude but then remains almost unchanged up to Re $= 10^4$, the highest value used in the calculations (Fig. 2).

The instability involving partial jet detachment occurs in several stages, which somewhat resemble those for plane wall jets in ordinary fluids [15]. Here, the quasi-2D behavior is enforced by the magnetic field which elongates flow structures in its direction. The CW-rotating vortices are attracted to the inner-wall region being promoted by high shear. The CCW-rotating ones are ejected into the outer jet region. The CW-rotating vortices merge and, by gaining momentum from the mean shear form a large CW-rotating vortex shown with dashed lines in Fig. 4(c). The front of this vortex is quite intense leading to the sweep of the fluid from the core towards the wall. This structure is followed by a strong burst of the fluid from the outer jet region into the core accompanied by the partially merged CCW-rotating vortices. The importance of the sweep is evident in Fig. 5 where the third-order moment $\bar{u}_1'^3$ shows a strong recirculation between the wall and the inflexion line in the mean velocity profile.

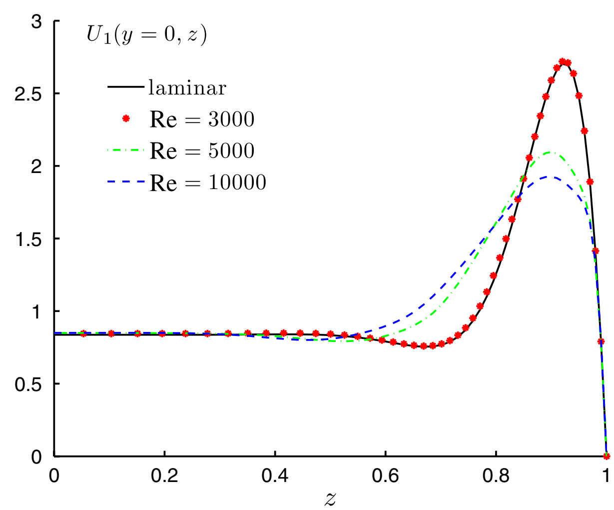

FIG. 3 (color online). Mean axial velocity profiles for several values of Re.

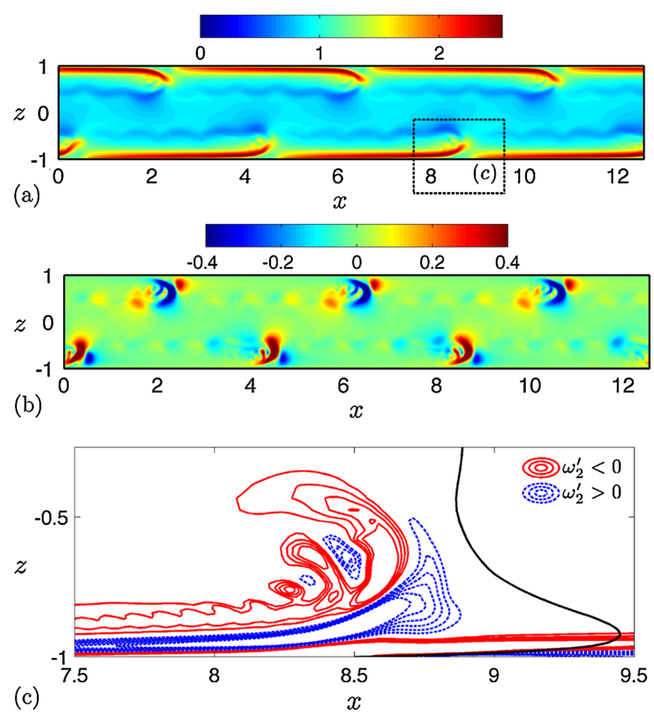

FIG. 4 (color online). Instantaneous contours of axial component of (a) the total axial velocity u_1 and (b) the transverse disturbance velocity u_3' for Re $= 5000$. (c) Instantaneous isolines of the y component of the disturbance vorticity $\omega_2' = (\mathbf{\nabla} \times \mathbf{u}')_2$ (red or gray and blue or dark gray lines) and mean velocity profile (black line). (c) is limited to the dashed box shown in (a).

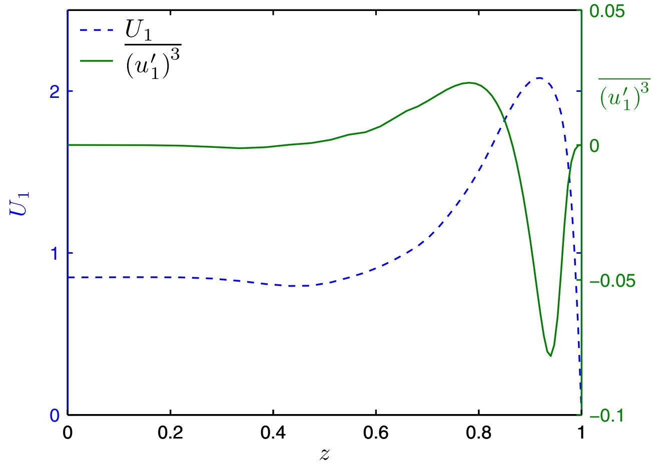

FIG. 5 (color online). Third-order moment $\bar{u}_1'^3$ compared to mean velocity profile for Re = 5000.

Figure 6 shows small-scale coherent structures in the outer jet region as defined by the region of negative λ_2, the second largest eigenvalue of the symmetric tensor $\mathbf{S}^2 + \mathbf{\Omega}^2$ [16]. Here $\mathbf{S}$ and $\mathbf{\Omega}$ are, respectively, the symmetric and antisymmetric parts of the velocity gradient tensor $\nabla\mathbf{u}$. It is seen that the structures are quasi–two dimensional (Q2D), nearly aligned with the magnetic field. However, recirculation of the mean flow in the duct cross section, through (U_2, U_3) does take place with 2% intensity of the peak of U_1 for Re = 5000 and 2.5% for Re = 10 000. Thus we conclude that the instability occurs in a Q2D manner with a certain increase in the three dimensionality in the sweep and burst regions. We leave the detailed analysis of the mechanism of instability for the future.

To summarize, two types of instabilities of jets have been identified in the simulation of an MHD flow in a square duct with thin conducting walls. The first instability occurs in the form of TW vortices, while the second is associated with the formation of a large-scale structure which involves sweeps and bursts of fluid at the walls parallel to the magnetic field and a partial detachment of the jets from the walls.

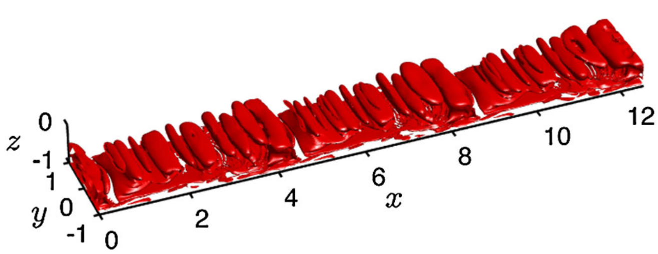

FIG. 6 (color online). Coherent structures in the outer jet region for Re = 5000, represented by isosurfaces of $\lambda_2 = -0.015$.

It should be noted that the second type of instability may have been observed in the experiments [9,10] where a sudden increase in the energy of perturbations by an order of magnitude at certain values of Re has been reported. However, owing mainly to the higher values of Ha and Re and to insufficient data in these experiments, direct comparison with our results has not been possible.

Overall, the instability in duct flows is expected to be very sensitive to the values of Re, as shown here, but also to Ha and c as demonstrated in Ref. [11], possibly leading to more types of instability and transition scenarios. Far more detailed studies are necessary to gain better understanding of MHD flows in ducts.

This work was conducted as part of a EURYI scheme grant [17]. M. K. is supported by F. R. I. A—Belgium. Large-scale calculations have been performed at a high performance cluster based at the Faculty of Engineering and Computing of Coventry University. The authors are indebted to Applied Mathematics Research Centre of Coventry University for providing this opportunity.

*mkinet@ulb.ac.be

[1] L. Bühler, in *Magnetohydrodynamics—Historical Evolution and Trends*, edited by S. Molokov, R. Moreau, and H. K. Moffatt (Springer, New York, 2007), pp. 171–194.
[2] D. S. Krasnov, E. Zienicke, O. Zikanov, T. Boeck, and A. Thess, J. Fluid Mech. **504**, 183 (2004).
[3] T. Boeck, D. Krasnov, A. Thess, and O. Zikanov, Phys. Rev. Lett. **101**, 244501 (2008).
[4] R. Moreau and S. Molokov, in Ref. [1], pp. 155–170.
[5] J. C. R. Hunt, J. Fluid Mech. **21**, 577 (1965).
[6] S. Molokov, Eur. J. Mech. B, Fluids **12**, 769 (1993).
[7] A. L. Ting, J. S. Walker, T. J. Moon, C. B. Reed, and B. F. Picologlou, Int. J. Eng. Sci. **29**, 939 (1991).
[8] C. B. Reed and B. F. Picologlou, Fusion Technol. **15**, 705 (1989).
[9] U. Burr, L. Barleon, U. Müller, and A. Tsinober, J. Fluid Mech. **406**, 247 (2000).
[10] L. Bühler and S. Horanyi, Fusion Eng. Des. **84**, 518 (2009).
[11] J. Priede, S. Aleksandrova, and S. Molokov, J. Fluid Mech. (to be published).
[12] K. Mahesh, G. Constantinescu, S. Apte, G. Iaccarino, F. Ham, and P. Moin, in *Annual Research Briefs* (Center for Turbulence Research, NASA Ames/Stanford University, Stanford, 2002), pp. 115–142.
[13] F. Ham, G. Iaccarino, in *Annual Research Briefs* (Center for Turbulence Research, NASA Ames/Stanford University, Stanford, 2004), pp. 3–14.
[14] M. J. Ni, R. Munipalli, P. Huang, N. B. Morley, and M. A. Abdou, J. Comput. Phys. **227**, 205 (2007).
[15] R. A. Bajura and M. R. Catalano, J. Fluid Mech. **70**, 773 (1975).
[16] J. Jeong and F. Hussain, J. Fluid Mech. **285**, 69 (1995).
[17] See http://www.esf.org/euryi.